Published in final edited form as:
Science. 2011 April 22; 332(6028): 478–484. doi:10.1126/science.1199214.

The Growth Factor Progranulin Binds to TNF Receptors and Is Therapeutic Against Inflammatory Arthritis in Mice

Wei Tang[1,2,*], **Yi Lu**[1,2,*], **Qing-Yun Tian**[1,*], **Yan Zhang**[1], **Feng-Jin Guo**[1,†], **Guang-Yi Liu**[1], **Nabeel Muzaffar Syed**[1], **Yongjie Lai**[1], **Edward Alan Lin**[1], **Li Kong**[1], **Jeffrey Su**[3], **Fangfang Yin**[4,‡], **Ai-Hao Ding**[4], **Alexandra Zanin-Zhorov**[5], **Michael L. Dustin**[5], **Jian Tao**[6], **Joseph Craft**[6], **Zhinan Yin**[7], **Jian Q. Feng**[8], **Steven B. Abramson**[9], **Xiu-Ping Yu**[2], and **Chuan-ju Liu**[1,10,§]

[1] Department of Orthopaedic Surgery, New York University School of Medicine and NYU Hospital for Joint Diseases, New York, NY 10003, USA

[2] Institute of Pathogenic Biology, Shandong University School of Medicine, Jinan, China

[3] Cytovance Biologics, Oklahoma City, OK 73104, USA

[4] Department of Microbiology and Immunology, Weill Medical College of Cornell University, New York, NY 10065, USA

[5] Department of Pathology, New York University School of Medicine, New York, NY 10016, USA

[6] Section of Rheumatology, Department of Medicine, Yale University School of Medicine, New Haven, CT 06520, USA

[7] College of Life Sciences, Nankai University, Tianjin 300071, China

[8] Baylor College of Dentistry, Texas A&M Health Science Center, Dallas, TX 75246, USA

[9] Division of Rheumatology, New York University School of Medicine and NYU Hospital for Joint Diseases, New York, NY 10003, USA

[10] Department of Cell Biology, New York University School of Medicine, New York, NY 10016, USA

Abstract

The growth factor progranulin (PGRN) has been implicated in embryonic development, tissue repair, tumorigenesis, and inflammation, but its receptors remain unidentified. We report that PGRN bound directly to tumor necrosis factor receptors (TNFR), and disturbed the TNFα/TNFR interaction. PGRN-deficient mice were susceptible to collagen-induced arthritis, and administration of PGRN reversed inflammatory arthritis. Atsttrin, an engineered protein composed of three PGRN fragments, exhibited selective TNFR binding. PGRN and Atsttrin prevented inflammation in multiple arthritis mouse models and inhibited TNFα-activated intracellular signaling. Collectively, these findings demonstrate that PGRN is a ligand of TNFR, an antagonist

§To whom correspondence should be addressed. chuanju.liu@med.nyu.edu.
*These authors contributed equally to this work.
†Present address: Chongqing Medical University, Chongqing, 400016, China.
‡Present address: SRI International, 333 Ravenswood Avenue, Menlo Park, CA 94025, USA.

Supporting Online Material
www.sciencemag.org/cgi/content/full/science.1199214/DC1
Materials and Methods
Figs. S1 to S19
Table S1
References

of TNFα signaling and plays a critical role in the pathogenesis of inflammatory arthritis in mice. They also suggest new potential therapeutic interventions for various TNFα-mediated pathologies and conditions, including rheumatoid arthritis.

Progranulin (PGRN), also known as granulin epithelin precursor (GEP), PC-cell-derived growth factor (PCDGF), proepithelin, and acrogranin, is an autocrine growth factor. PGRN contains seven-and-a-half repeats of a cysteine-rich motif (CX5–6CX5CCX8CCX6CCXDX2HCCPX4CX5–6C) in the order P-G-F-B-A-C-D-E, where A-G are full repeats and P is the half-motif (1). PGRN is expressed in rapidly cycling epithelial cells, leukocytes, neurons (2), and chondrocytes (3). Some human cancers also express PGRN and PGRN contributes to tumorigenesis in breast cancer, ovarian carcinoma, and multiple myeloma (2, 4). PGRN plays a critical role in a variety of physiologic and disease processes, including early embryogenesis (5), wound healing (6), inflammation (7, 8), host defense (9) and cartilage development and degradation (3, 10–12). PGRN also functions as a neurotrophic factor (13) and mutations in the *Grn* gene cause frontotemporal dementia (14–16). Despite such a variety of roles, efforts to exploit the actions of PGRN and understand the mechanisms involved have been significantly hampered by our inability to identify its binding receptor(s) (2).

TNFα/TNFR signaling has received great attention due to its position at the apex of the proinflammatory cytokine cascade and its dominance in the pathogenesis of various disease processes, and in particular, autoimmune disorders (17). TNFα blockers including etanercept (Enbrel), infliximab (Remicade), and adalimumab (Humira), are effective anti-inflammatory therapies (18, 19). TNFR1 is expressed ubiquitously, whereas TNFR2 expression is tightly regulated and found predominantly in hematopoietic cells (20). In a search for PGRN-associated proteins we screened a yeast two-hybrid (Y2H) cDNA library using the construct pDBleu-PGRN (a.a.21-588) encoding PGRN lacking signal peptide as bait, and isolated 12 positive clones among 2.5 millions clones. Sequencing data showed that two of them were cell surface TNFR2 (TNFRSF1B/CD120b). The interaction between PGRN and TNFR2 in yeast was then verified by repeating the Y2H assay. The interaction between PGRN and TNFR in human chondrocytes was demonstrated by co-immunoprecipitation (Co-IP) (Fig. 1A, fig. S1A). Recombinant human PGRN (rhPGRN) demonstrated dose-dependent binding and saturation to liquid-phase the extracellular domains of TNFR1 and TNFR2 (fig. S1B). Kinetic binding studies revealed that rhPGRN exhibited comparable binding affinity for TNFR1 and TNFR2 and had higher affinity for TNF receptors, especially TNFR2, when compared to TNFα (Fig. 1B).

The finding that PGRN directly binds to TNFR prompted us to determine whether PGRN affected the TNFα/TNFR interaction. rhPGRN demonstrated dose-dependent inhibition of TNFα binding to TNFR1 and TNFR2 (Fig. 1, C and D), which suggested that PGRN may act as a physiological antagonist of TNFα signaling. Indeed, PGRN potently inhibits TNF-mediated neutrophil activation (8) and cartilage degradation (10). We observed a significant increase in TNFα-stimulated hydrogen peroxide in neutrophils and nitric oxide in bone marrow derived macrophages (BMDMs) from PGRN-deficient mice (Fig. 1, E and F). We have previously reported that TNFα induces the degradation of COMP (21), a prominent noncollagenous component of cartilage that plays an important role in stabilizing the cartilage matrix (22, 23) and is heavily degraded in both osteoarthritis and rheumatoid arthritis (21, 24, 25). Using the same model system, we observed that deletion of PGRN results in a marked increase in TNFα-induced COMP degradation (fig. S2).

In order to determine whether PGRN affects TNFα signaling in human cells, we next examined the possibility that treatment of human regulatory T cells (Treg; phenotypically $TNFR2^{+}$ $TNFR1^{-}$ (26)) with PGRN may protect Treg cells from negative regulation by

TNFα (26, 27). PGRN protected Treg from a negative regulation by TNFα (fig. S3) and promoted the differentiation of Treg from naïve T cells (fig. S4). Furthermore, TNFα up-regulated, whereas PGRN down-regulated interferon (IFN)-γ secretion in effector T cells (Teff) (fig. S5). TNFR1 blocking antibodies largely inhibited TNFα-induced upregulation of IFNγ secretion, but did not affect PGRN-mediated suppression; in contrast, TNFR2 blocking antibodies abolished PGRN-mediated downregulation of IFNγ production (fig. S5). These data indicate that the regulation of TNFα and PGRN on Teff cells primarily depend on TNFR1 and TNFR2, respectively.

To examine the role of endogenous PGRN during inflammation in vivo, we investigated the clinical and histopathological features of PGRN-deficient *C57BL/6* mice ($Grn^{-/-}$) in a mouse model of collagen-induced arthritis (CIA) (28, 29), which shares both immunological and pathological features with human rheumatoid arthritis. $Grn^{-/-}$ mice developed more severe inflammatory arthritis and increased bone and joint destruction as compared with their control littermates (Fig. 2, A and B). We also observed a significant increase in the arthritis severity score (Fig. 2C), a reduced time to disease onset and a greater incidence of arthritis in $Grn^{-/-}$ mice compared to control mice (Fig. 2D). Histological and quantitative analysis of whole ankle joints demonstrated a significant increase in synovitis, pannus formation, and destruction of bone and cartilage in $Grn^{-/-}$ mice, compared with controls (Fig. 2E). Other hallmarks of arthritis, such as loss of matrix staining in the articular cartilage and an increase in bone-resorbing osteoclasts, were exacerbated in $Grn^{-/-}$ mice (fig. S6, A and B).

To determine whether the inflammatory arthritis of collagen II-challenged PGRN-deficient mice can be neutralized by recombinant PGRN, we administrated rhPGRN to these PGRN-deficient mice for 11 weeks [supporting online materials (SOM) Materials and Methods]. rhPGRN completely blocked disease progression (Fig. 2F). No visible symptoms of CIA were observed in any individual mouse, which was manifested by both a 0% incidence and an arthritis score of “0” in PGRN-deficient mice treated with rhPGRN (Fig. 2, G and H). rhPGRN also significantly inhibited synovitis, pannus formation, tissue destruction (fig. S6C), and the loss of cartilage matrix (fig. S6D). Notably, the number of osteoclasts was reduced in PGRN-deficient mice treated with rhPGRN when compared to untreated PGRN-deficient mice (fig. S6E). Collectively, these data suggest that the loss of PGRN expression in vivo results in enhanced susceptibility to collagen induced arthritis, which can be entirely reversed by the administration of recombinant PGRN.

To determine whether the anti-inflammatory actions of PGRN occur through the suppression of TNFα signaling in vivo, we deleted the gene that encodes PGRN in mice that express a human TNFα transgene (TNF-Tg) (30). TNF-Tg mice develop an inflammatory arthritis phenotype spontaneously (30, 31). We generated TNF-Tg/$Grn^{+/-}$ and TNF-Tg/$Grn^{-/-}$ mice and found that the deletion of PGRN hastened the onset of arthritis and resulted in a worse clinical score in a gene dosage-dependent manner (Fig. 3, A and B). 12-week-old TNF-Tg/$Grn^{-/-}$ and TNF-Tg/$Grn^{+/-}$ mice developed severe swelling and joint deformation (fig. S7A), significantly increased synovitis, pannus formation, destruction of the wrist joints (fig. S7B), and loss of cartilage matrix (fig. S7C). Overexpression of TNFα resulted in prominent calvarial osteoclast activity of TNF-Tg mice, and deletion of PGRN further enhanced this activity (fig. S7D). These results suggest that PGRN may also be a negative regulator of TNFα-induced osteoclastogenesis and a mediator of bone integrity during the inflammatory process.

Next, we sought to examine the effects of applying recombinant human PGRN to TNF-Tg mice. We administered rhPGRN (SOM Materials and Methods) to TNF-Tg mice with established mild arthritis. Treatment with rhPGRN resulted in the elimination of any visual

signs of arthritis (Fig. 3C) and a reduced arthritis severity score (Fig. 3D). To confirm that these effects were due to the inhibitory effects of PGRN, we discontinued rhPGRN administration and continued to evaluate the TNF-Tg mice for signs of arthritis. At 7 days after the cessation of rhPGRN treatment, signs of arthritis began to develop (Fig. 3D). In contrast, application of rhPGRN to TNF-Tg mice in the phosphate buffered saline (PBS)-treated group resulted in a marked reduction of severe arthritis signs. Taken together, these data suggest that PGRN may exert its anti-inflammatory effects through inhibition of TNF/TNFR signaling in vivo.

To identify the domains of PGRN required for its interaction with TNF receptors, we constructed cDNA segments encoding a series of PGRN mutants and analyzed their interactions with TNFR2 using Y2H assays. No single granulin unit (fig. S8A) or linker region (fig. S8B) was able to bind to TNFR2, suggesting that the binding domain of PGRN may span granulin unit and linker. We first expressed each granulin with its immediately adjacent downstream or upstream linker and observed only weak binding of granulin F-P3, P4-granulin A and P5-granulin C to TNFR2 (fig. S9, A and B). We then linked all three fragments identified above to generate an engineered mutant (referred to as FAC) (fig. S10A) which exhibited an even stronger binding affinity to TNFR2 than PGRN. F, A and C are known to be the granulin domains most capable of independent folding, and each of domain has N and C terminal subdomains that are structurally independent (32). By deleting ever greater portions of each of the granulin domains of FAC we determined a mutant composed of half units of granulins A, C and F plus linkers P3, P4 and P5 appears to be the "minimal" engineered molecule that retains affinity to TNFR2 (fig. S10). This molecule was referred to as Atsttrin (Antagonist of TNF/TNFR Signaling via Targeting to TNF Receptors). Y2H assay revealed that PGRN associated weakly with other members of TNFR subfamily, whereas Atsttrin selectively interacted with TNFR1 and TNFR2 (fig. S11). Atsttrin was expressed in bacteria as a GST fusion protein, purified on glutathione agarose resin, and eluted using Xa factor (there is a Xa factor cleavage site between GST and Atsttrin) (fig. S12A). Reverse phase HPLC showed high purity (~90%), indicating one major isoform of Atsttrin (fig. S12B). 5 of 17 cysteine residues within Atsttrin molecule exist as free thiols. When compared to TNFα, recombinant Atsttrin exhibited higher binding affinity for TNFR2, but lower affinity for TNFR1 (Fig. 4A). Atsttrin demonstrated dose-dependent inhibition of the interaction between TNFα and TNFR1/TNFR2 (Fig. 4, B and C). Furthermore, Atsttrin also inhibited the binding of lymphotoxin α (LTα) to TNFR1 and TNFR2 (fig. S13).

Atsttrin could inhibit several downstream events of TNF/TNFR signaling. Atsttrin inhibited TNFα-dependent hydrogen peroxide production in neutrophils and nitric oxide production in BMDMs in a dose-dependent manner (fig. S14, A and B). Even at high dosages, Atsttrin did not exhibit any cytotoxic effects (fig. S14C). Furthermore, Atsttrin effectively blocked TNFα-mediated death of rhabdomyosarcoma A673/6 cells (fig. S14D). To examine the effects of TNFα on osteoclastogenesis, we administered TNFα to M-CSF–dependent mouse BMDMs, which induced differentiation of these cells into osteoclasts. Co-administration of Atsttrin led to a significantly lower number of TRAP-positive osteoclasts, when compared to the control (fig. S14E), and reduced the number and mean size of bone resorption pits (fig. S14F).

We next determined the impact of PGRN and Atsttrin in two different mouse models of rheumatoid arthritis: collagen antibody–induced arthritis (CAIA) and collagen-induced arthritis (CIA). In the CAIA model, we challenged mice with a cocktail of anti-collagen antibodies and LPS and then randomized them to treatment with rhPGRN, Atsttrin, or PBS, starting on day 1. Administration of either rhPGRN or Atsttrin resulted in reduced disease severity in the CAIA model, and both agents significantly delayed the progression of

arthritis (Fig. S15A). Furthermore, Atsttrin was more effective than rhPGRN in delaying the onset of inflammation (Fig. S15A). We analyzed paw thickness of the Atsttrin-treated group and noticed a significant decrease in size to a nearly normal range, when compared with the PBS-treated group (Fig. S15B). Histological analysis of ankle joints indicated a significant decrease in inflammatory cell infiltration, tissue destruction, bone erosion, and loss of cartilage matrix in rhPGRN- and Atsttrin-treated CAIA mice (Fig. S15C).

In the CIA model, mice treated with rhPGRN or Atsttrin (SOM Materials and Methods) demonstrated markedly reduced joint swelling, erythema, and gross deformity compared to PBS-treated controls, with Atsttrin-treated mice bearing marked similarity to normal mice (Fig. 5A). PGRN, Atsttrin and etanercept effectively prevented the development of arthritis, as evidenced by a decreased arthritis severity score and lower incidence of disease (Fig. 5, B and C). Atsttrin was more effective than either rhPGRN or etanercept in this model, and completely prevented the onset of inflammation. Histological and quantitative analysis of the tarsal joints revealed essentially normal articular anatomy in the rhPGRN and Atsttrin treatment groups. In contrast, a robust infiltration of immune cells, tissue destruction, bone erosion, and loss of cartilage matrix were observed in the PBS-treated control mice (Fig. 5D and fig. S16A). Micro-CT images revealed gross bone damage in the PBS-treated CIA mice, but not in the rhPGRN- or Atsttrin-treated groups (fig. S16B). Furthermore, osteoclast activity was undetectable in both rhPGRN and Atsttrin treated CIA mice (fig. S16C). Mice treated with rhPGRN or Atsttrin also had significantly decreased serum levels of proinflammatory cytokines interleukin (IL)-1β and IL-6, and COMP, and elevated levels of anti-inflammatory cytokines IL-10 and IL-13, when compared with control mice (fig. S16, D and E).

To determine the pharmacokinetic profile of Atsttrin, we first generated an anti-serum by immunizing mice with recombinant Atsttrin. The specificity of anti-Atsttrin antibodies was confirmed by immunoblotting (fig. S17A). An indirect ELISA using anti-Atsttrin antibody was then established (fig. S17B), and the pharmacokinetic profile of Atsttrin in mice was examined. Atsttrin was well absorbed following intraperitoneal administration and demonstrated high stability with a half-life of about 120 hours (fig. S17, C and D). From these data, the pharmacokinetic parameters and availability were then calculated (Table S1). On the basis of these results, we subsequently investigated the optimal dose of Atsttrin required to prevent CIA using a long dosing interval by injecting collagen-induced mice with Atsttrin once per week. The anti-inflammatory actions of Atsttrin displayed dose-dependency (fig. S18A), and administration of Atsttrin at a dose of 0.5 mg/kg body weight or higher completely prevented the induction of arthritis. We also found that a single dose of Atsttrin (10 mg/kg) could effectively delay the onset of inflammation for approximately three weeks (fig. S18B). Taken together, these findings suggest that PGRN and its derived Atsttrin can effectively prevent CIA in mice. We then examined the therapeutic efficacy of Atsttrin in treating already established CIA. Administration of Atsttrin once per week effectively inhibited or reversed disease progression in a dose-dependent manner (Fig. 5E). We also confirmed the therapeutic efficacy of Atsttrin in a TNF-Tg mouse model. Consistent with the results observed in the CIA model, the administration of Atsttrin markedly suppressed arthritis progression, and notably eliminated signs of inflammation (fig. S19). Signs of inflammation returned following the cessation of Atsttrin treatment (fig. S19B).

To define the contributions of TNFR1 and TNFR2 in the therapeutic effects of Atsttrin, we compared the therapeutic effects of Atsttrin on CIA in wildtype, and mice deficient in TNFR1 (Tnfrsf1a$^{-/-}$) or TNFR2 (Tnfrsf1b$^{-/-}$) (Fig. 5F). Atsttrin treatment was effective in both wildtype and Tnfrsf1a$^{-/-}$ mice in a dose-dependent fashion. In contrast, only the highest dose of Atsttrin (0.5mg/kg) exerted a significant effect in Tnfrsf1b$^{-/-}$ mice. These

data indicated that Tnfrsf1b$^{-/-}$ CIA mice are less sensitive to Atsttrin treatment, possibly because Atsttrin bound to TNFR2 with a higher affinity than to TNFR1 and there is a very different distribution and function between TNFR1 and TNFR2 in T cells (26, 27).

To explore further the anti-inflammatory mechanisms of PGRN and Atsttrin, we investigated the role of PGRN and Atsttrin in the TNFα-induced activation of IKK/IκB/NF-κB signaling. rhPGRN and Atsttrin blocked TNFα-induced phosphorylation of IKK and IκBα and the degradation of IκBα in BMDMs (Fig. 6A). We also found elevated IκBα phosphorylation in the tarsal joint articular cartilage of mice with CIA, which was abolished by treatment with rhPGRN or Atsttrin (Fig. 6B). rhPGRN- or Atsttrin treatment of BMDMs impaired TNFα-induced NF-κB nuclear translocation, NF-κB binding to the IκBα promoter and activation of gene expression by NF-κB (Fig. 6, C–F) (33). rhPGRN and Atsttrin also inhibited the TNFα-induced phosphorylation of p38, JNK and ERK1/2, mitogen activated protein kinase (MAPK) family members known to play an important role in TNFα-mediated inflammation (Fig. 6G). While Atsttrin completely blocked the TNFα-induced phosphorylation of ERK1/2, the presence of rhPGRN only resulted in a partial inhibition of this pathway. This may not be surprising, however, because PGRN itself has been previously shown to activate ERK1/2 signaling (3). Taken together, these results demonstrate that PGRN and Atsttrin inhibit TNFα-induced intracellular signaling pathways.

Collectively, our findings support the notion that PGRN is a key regulator of inflammation and that PGRN may mediate its anti-inflammatory effects, at least in part, by blocking TNF binding to its receptors. Whether this mechanism accounts for all of the anti-inflammatory effects we observed remains to be further delineated.

During inflammation, neutrophils and macrophages release proteases which digest PGRN into individual 6 kDa granulin units, which are actually pro-inflammatory and can neutralize the antiinflammatory effects of intact PGRN (7, 8). PGRN's anti-inflammatory actions are protected by its binding proteins, which include the secretory leukocyte protease inhibitor (8) and apolipoprotein A1 (34), both of which bind to PGRN and protect it against proteolytic degradation. Consistent with these observations, we found that the PGRN-derived protein, Atsttrin, exhibits highly potent anti-inflammatory activity which surpasses PGRN itself, in vivo. This occurred despite the observation that PGRN binds to TNFR with a higher affinity than Atsttrin. This may be because Atsttrin contains only partial granulin units and would not be expected to release any intact proinflammatory granulin units upon exposure to PGRN-converting enzymes such as elastase (8), proteinase-3 (7) and ADAMTS-7 (35). Moreover, Atsttrin exhibited a substantially longer half-life (~120 hours) when compared to PGRN (~40 hours). The identification of PGRN and the PGRN-derived protein, Atsttrin, as antagonists of TNFR may lead to innovative therapeutics for various pathologies and conditions, such as rheumatoid arthritis.

Supplementary Material

Refer to Web version on PubMed Central for supplementary material.

Acknowledgments

We thank P. Lengyel, J. Vilcek and T. C. Caskey for critical reading and comments. G. Wisniewski for assisting with the CIA model, M. E. Dorf and A. Mukundan for reagents, A. Martin and J. Quinn for assistance in Surface Plasmon Resonance assay. This work was funded by NIH grants AR050620, AR053210 (to C. J. L), GM061710 (to A. H. D), AI43542 (to M.L.D) and AR040072 (to J. C.), a grant from Arthritis National Research Foundation (to C. J. L), and a National Outstanding Young Scientist Award of NSFC 30725015 (to Z. N. Y). Patents have been filed by NYU that claim peptides targeting TNF family receptors and antagonizing TNF action, compositions, methods and uses thereof [WO/2010/120374 (C. J. L), PCT/US2010/001137 (C. J. L)]. TNFR2 (TNFRSF1B/CD120b) Accession #: NM_130426. A full list of author contributions is available in the SOM.

References and Notes

1. Hrabal R, Chen Z, James S, Bennett HP, Ni F. Nat Struct Biol. 1996; 3:747. [PubMed: 8784346]
2. Bateman A, Bennett HP. Bioessays. 2009; 31:1245. [PubMed: 19795409]
3. Feng JQ, et al. FASEB J. 2010; 24:1879. [PubMed: 20124436]
4. He Z, Bateman A. J Mol Med. 2003; 81:600. [PubMed: 12928786]
5. Daniel R, He Z, Carmichael KP, Halper J, Bateman A. J Histochem Cytochem. 2000; 48:999. [PubMed: 10858277]
6. He Z, Ong CH, Halper J, Bateman A. Nat Med. 2003; 9:225. [PubMed: 12524533]
7. Kessenbrock K, et al. J Clin Invest. 2008; 118:2438. [PubMed: 18568075]
8. Zhu J, et al. Cell. 2002; 111:867. [PubMed: 12526812]
9. Yin F, et al. J Exp Med. 2010; 207:117. [PubMed: 20026663]
10. Guo F, et al. Arthritis Rheum. 2010; 62:2023. [PubMed: 20506400]
11. Xu K, et al. J Biol Chem. 2007; 282:11347. [PubMed: 17307734]
12. Liu CJ. Nat Clin Pract Rheumatol. 2009; 5:38. [PubMed: 19098927]
13. Van Damme P, et al. J Cell Biol. 2008; 181:37. [PubMed: 18378771]
14. Baker M, et al. Nature. 2006; 442:916. [PubMed: 16862116]
15. Cruts M, et al. Nature. 2006; 442:920. [PubMed: 16862115]
16. Van Deerlin VM, et al. Nat Genet. 2010; 42:234. [PubMed: 20154673]
17. Aggarwal BB. Nat Rev Immunol. 2003; 3:745. [PubMed: 12949498]
18. Netterwald J. Nat Biotechnol. 2009; 27:495. [PubMed: 19513037]
19. Taylor PC. Nat Clin Pract Rheumatol. 2009; 5:126. [PubMed: 19252515]
20. Luo D, et al. Am J Pathol. 2006; 169:1886. [PubMed: 17071609]
21. Luan Y, et al. Osteoarthritis Cartilage. 2008; 16:1413. [PubMed: 18485748]
22. Briggs MD, et al. Nature. 1995; 10:330.
23. Hecht JT, et al. Nat Genet. 1995; 10:325. [PubMed: 7670471]
24. Liu CJ, et al. FASEB J. 2006; 20:988. [PubMed: 16585064]
25. Liu CJ, et al. J Biol Chem. 2006; 281:15800. [PubMed: 16611630]
26. Valencia X, et al. Blood. 2006; 108:253. [PubMed: 16537805]
27. Zanin-Zhorov A, et al. Science. 2010; 328:372. [PubMed: 20339032]
28. Feldmann M, Maini RN. Nat Med. 2003; 9:1245. [PubMed: 14520364]
29. Deng GM, Zheng L, Chan FK, Lenardo M. Nat Med. 2005; 11:1066. [PubMed: 16170321]
30. Keffer J, Probert L, Cazlaris H, Georgopoulos SK, Kioussis SD, Kollias G. EMBO J. 1991; 10:4025. [PubMed: 1721867]
31. Thwin MM, et al. Arthritis Res Ther. 2004; 6:R282. [PubMed: 15142275]
32. Tolkatchev D, et al. Protein Sci. 2008; 17:711. [PubMed: 18359860]
33. Tian B, Nowak DE, Jamaluddin M, Wang S, Brasier AR. J Biol Chem. 2005; 280:17435. [PubMed: 15722553]
34. Okura H, et al. J Atheroscler Thromb. 2007
35. Bai XH, et al. Mol Cell Biol. 2009; 29:4201. [PubMed: 19487464]

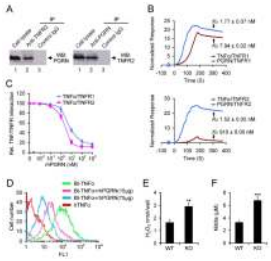

Fig. 1.

PGRN directly binds to TNFR and antagonizes TNFα actions. (**A**) PGRN interacts with TNFR2 in chondrocytes (Co-IP assay). The cell lysates of human chondrocytes were incubated with anti-PGRN, anti-TNFR2 or control IgG antibodies, and bound protein was examined by Western blotting with the corresponding antibodies, as indicated. (**B**) FastStep Kinetic Assay for binding of PGRN and TNFα to TNFR1 and TNFR2. Samples were injected using FastStep injection, and dissociation of analyte-ligand complexes was monitored. K_D for each interaction is indicated. (**C**) PGRN inhibits the binding of TNFα to TNFR1 and TNFR2 (solid phase binding). Microtiter plate coated with TNFα was incubated with TNFR1 or TNFR2 in the presence of various amounts of rhPGRN, and the bound TNFR to TNFα was detected by corresponding antibodies. Values are mean ± s.d. (**D**) Flow cytometry analysis of Raw264.7 cells after staining with 50 ng biotinylated human TNF-α (Bt-TNFα) and different doses of rhPGRN pretreatment. (**E**) PGRN deletion potentiates TNFα-induced H_2O_2 production (neutrophil activation). Wild type (WT) or PGRN-deficient (KO) neutrophils were treated with TNFα, and H_2O_2 production was measured. Values are mean ± s.d. **P <0.01; n=4. (**F**) PGRN deletion potentiates TNFα-induced nitrite production in bone marrow derived macrophages (BMDMs). M-CSF pretreated wild type (WT) or PGRN-deficient (KO) BMDMs were incubated with TNFα, and the supernatants were tested for NO production. Values are mean ± s.d. ***P <0.001; n=4.

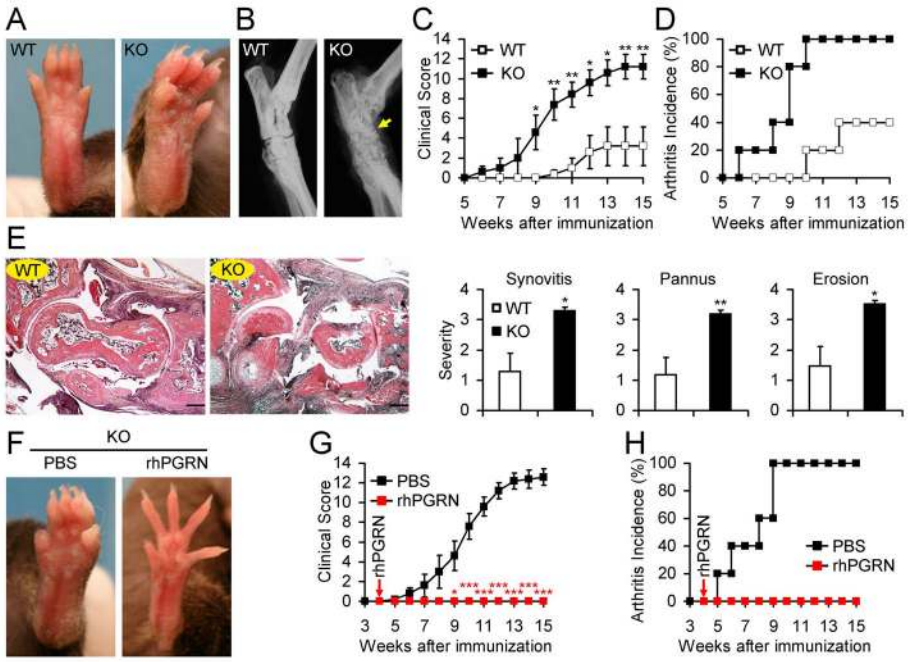

Fig. 2.

PGRN-deficient mice are highly susceptible to collagen-induced arthritis, and administration of PGRN reverses the severe inflammatory arthritis seen in collagen-challenged PGRN-deficient mice. (**A**) Paws of wild type (WT) and *Grn*$^{-/-}$ (KO) mice derived from *C57BL/6* (*n*=10/group) immunized with collagen II for 15 weeks. (**B**) Radiography of ankle joints of WT and KO collagen II-immunized mice. Arrow indicates areas of severe joint destruction in PGRN-deficient CIA mice. (**C**) Clinical arthritis scores in WT and KO mice with CIA. The data are presented as the mean clinical score ± s.e.m. **P*<0.05, ***P*<0.01 versus the control WT group. (**D**) Incidence of arthritis in the indicated groups. (**E**) H&E stained sections and evaluation of synovitis, pannus and erosion of ankle joints in WT and KO mice with CIA 15 weeks following primary immunization. Scale bar, 200μm. Values are mean ± s.d. **P*<0.05, ***P*<0.01 versus the control WT group. (**F**) Paws of KO mice treated with PBS or rhPGRN from 4 to 15 weeks following collagen II immunization. (**G**) Clinical arthritis scores in KO mice with CIA treated with PBS or rhPGRN (*n*=10/group). Data are presented as the mean clinical score ± s.e.m. ***P*<0.01, ****P*<0.001 versus the control PBS group. (**H**) Incidence of arthritis in each experimental group.

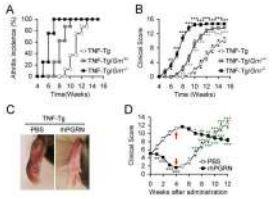

Fig. 3.

Deletion of PGRN exacerbates, whereas recombinant PGRN prevents, the spontaneous development of inflammatory arthritis in TNF transgenic mice. (**A**) Incidence of arthritis in TNF-Tg, TNF-Tg/$Grn^{+/-}$, and TNF-Tg/$Grn^{-/-}$, mice (n=8/group). (**B**) Clinical arthritis scores. Data are presented as the mean clinical score ± s.e.m. *P<0.05, **P<0.01 and ***P<0.001 versus the control TNF-Tg group. (**C**) Photographs of paws of TNF-Tg mice with mild arthritis treated with either PBS or rhPGRN for 4 weeks. (**D**) Effect of PGRN in TNF-Tg mice. TNF-Tg mice with established mild arthritis (Clinical score is around 5) were treated with PBS or rhPGRN (n=8/group). The treatment type was then switched between the two groups, and the switch time point is indicated with arrows. Development of arthritis was then scored. The data are presented as the mean clinical score ± s.e.m. The statistics were compared between untreated (PBS) and rhPGRN-treated group before the switch time point (black star). After that statistics were compared to the switch time point in each group (green star). *P<0.05, **P<0.01, ***P<0.001.

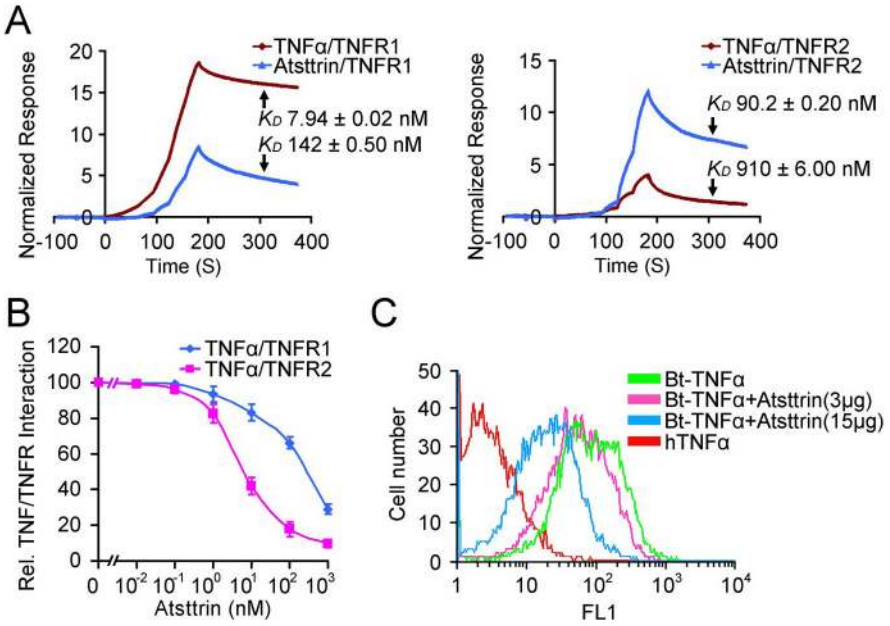

Fig. 4.

Atsttrin exhibits selective TNFR binding and inhibits TNFα/TNFR interactions. (**A**) FastStep Kinetic Assay for binding of Atsttrin and TNFα to TNFR1 and TNFR2. Samples were injected using FastStep injection, and dissociation of analyte-ligand complexes was monitored. K_D for each interaction was indicated. (**B**) Atsttrin inhibits the binding of TNFα to TNFR1 and TNFR2 (solid phase binding). Microtiter plate coated with TNFα was incubated with TNFR1 or TNFR2 in the presence of various amounts of Atsttrin, and the bound TNFR to TNFα was detected by corresponding antibodies. Values are mean ± s.d. (**C**) Flow cytometric analysis of Raw264.7 cells after staining with 50 ng biotinylated human TNFα (Bt-TNFα) in the presence of different doses of Atsttrin.

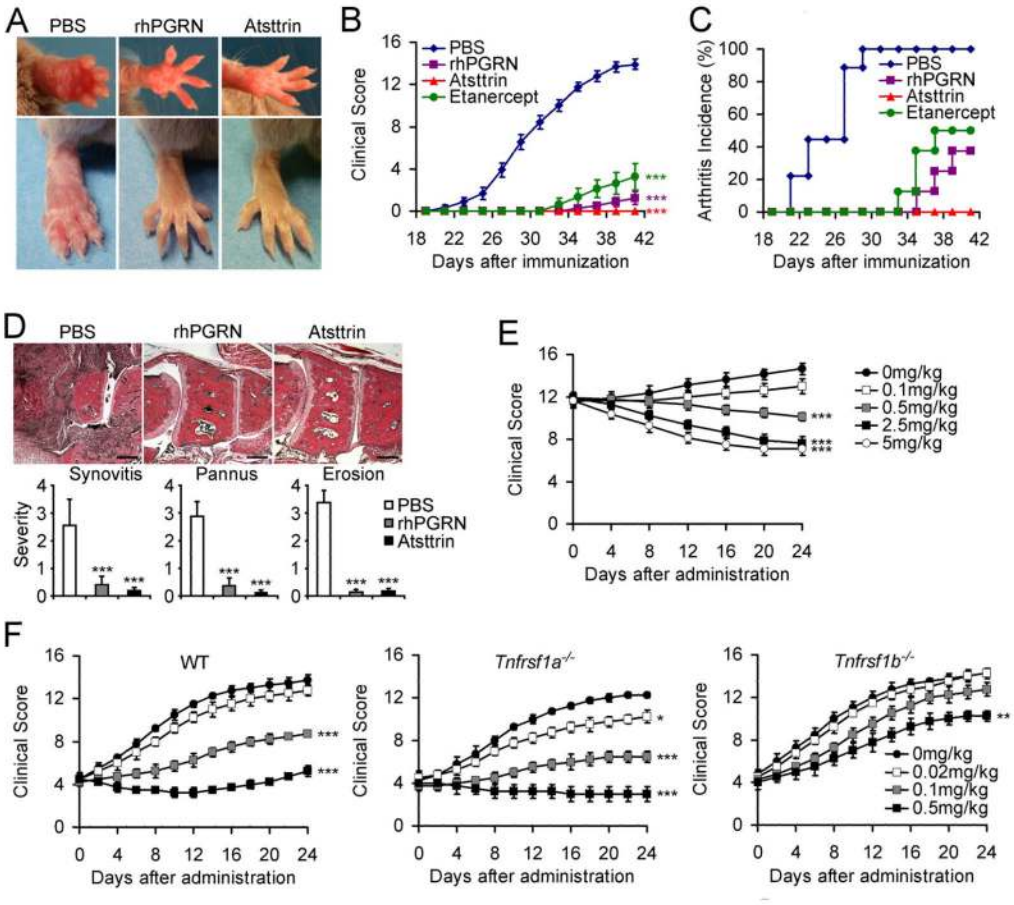

Fig. 5.

Effects of PGRN and Atsttrin in CIA. (**A**) Photographs of paws of CIA mice treated with PBS, rhPGRN, or Atsttrin. (**B**) Clinical arthritis scores in PBS (*n*=9), rhPGRN (*n*=8), Atsttrin (*n*=12) or Etanercept (*n*=8) treated CIA mice. Data are presented as the mean clinical score ± s.e.m. ***P<0.001 versus the control PBS group. (**C**) Incidence of arthritis in each treatment group. (**D**) H&E stained sections and evaluation of synovitis, pannus formation, and erosion of tarsal joints in CIA mice sacrificed at day 41 following primary immunization and treatment (starting day 19) with PBS, rhPGRN or Atsttrin. Scale bar, 200μm. Values are mean ± s.d. ***P<0.001 versus the control PBS group. (**E**) Therapeutic effects of Atsttrin in established CIA mice receiving intraperitoneal injections of indicated amounts of Atsttrin (mg per kg bodyweight once a week; *n*=8/group). Values are mean ± s.e.m. ***P<0.001 versus the group of Atsttrin at a dose of 0. (**F**) Therapeutic effects of Atsttrin in established CIA of wild type, *Tnfrsf1a*$^{-/-}$, *Tnfrsf1b*$^{-/-}$ mice. Atsttrin was administered at 0.02, 0.1or 0.5 mg per kg body weight once a week; *n*=8/group. Values are mean ± s.e.m. *P<0.05, **P<0.01, *** P<0.001 versus the 0mg/kg treatment group.

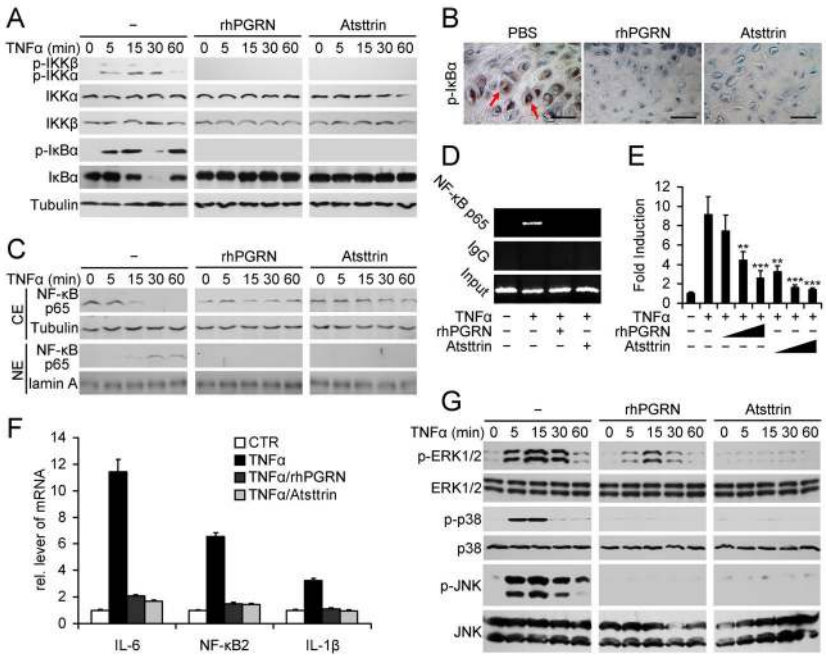

Fig. 6.

PGRN and Atsttrin inhibit TNFα-mediated activation of NF-κB and MAPK signaling. (**A**) BMDMs were incubated with TNFα in the presence or absence of rhPGRN or Atsttrin, and phosphorylation and expression of the indicated signaling molecules at various time points were determined by immunoblotting. Tubulin is shown as a loading control. (**B**) Immunohistochemistry for phosphorylated IκBα in the articular cartilage of CIA mice on day 41 following primary immunization and treatment with PBS, rhPGRN or Atsttrin. Arrows indicate phosphorylated IκBα. Scale bar, 25μm. (**C**) NF-κB amounts were analyzed by Western blotting with p65 antibody and assessed using cytoplasmic (CE) and nuclear (NE) extracts of TNFα-treated BMDMs in the presence and absence of rhPGRN or Atsttrin. Tubulin and lamin A serve as cytoplasmic and nuclear controls, respectively. (**D**) BMDMs were incubated with TNFα in the presence or absence of rhPGRN or Atsttrin for 6 hours, and analyzed by chromatin immunoprecipitation (ChIP) assay. (**E**) BMDMs transfected with the NF-κB-dependent reporter construct were incubated with TNFα (10 ng/ml) in the presence of increasing concentrations of rhPGRN or Atsttrin (0.1, 0.5, 2.5nM), and the luciferase activity was measured. Values are mean ± s.d. ***P*<0.01, ****P*<0.001 versus TNFα-stimulated cells. (**F**) The order change of mRNA expression relative to unstimulated cells, as assessed by real time PCR. (**G**) PGRN and Atsttrin inhibit TNFα-induced ERK1/2, p38 and JNK phosphorylation. BMDMs were stimulated with TNFα in the presence or absence of rhPGRN or Atsttrin. At the indicated time points, cell lysates were probed using specific antibodies against total and phosphorylated Erk1/2, p38, and JNK.